Title
Peroxiredoxin 6 suppresses ferroptosis in lung endothelial cells.

Authors
Torres-Velarde, Julia
Allen, Kaitlin
Salvador-Pascual, Andrea
et al.

Publication Date
2024-06-01

DOI
10.1016/j.freeradbiomed.2024.04.208

Peer reviewed

Published in final edited form as:

Free Radic Biol Med. 2024 June ; 218: 82–93. doi:10.1016/j.freeradbiomed.2024.04.208.

Peroxiredoxin 6 suppresses ferroptosis in lung endothelial cells

Julia María Torres-Velarde[1],
Kaitlin N. Allen[1],
Andrea Salvador-Pascual,
Roberto G. Leija,
Diamond Luong,
Diana Daniela Moreno-Santillán,
David C. Ensminger[2],
José Pablo Vázquez-Medina[*]
Department of Integrative Biology, University of California, Berkeley, USA

Abstract

Peroxiredoxin 6 (Prdx6) repairs peroxidized membranes by reducing oxidized phospholipids, and by replacing oxidized sn-2 fatty acyl groups through hydrolysis/reacylation by its phospholipase A_2 (aiPLA_2) and lysophosphatidylcholine acyltransferase activities. Prdx6 is highly expressed in the lung, and intact lungs and cells null for Prdx6 or with single-point mutations that inactivate either Prdx6-peroxidase or aiPLA_2 activity alone exhibit decreased viability, increased lipid peroxidation, and incomplete repair when exposed to paraquat, hyperoxia, or organic peroxides. Ferroptosis is form of cell death driven by the accumulation of phospholipid hydroperoxides. We studied the role of Prdx6 as a ferroptosis suppressor in the lung. We first compared the expression Prdx6 and glutathione peroxidase 4 (GPx4) and visualized Prdx6 and GPx4 within the lung. Lung Prdx6 mRNA levels were five times higher than GPx4 levels. Both Prdx6 and GPx4 localized to epithelial and endothelial cells. Prdx6 knockout or knockdown sensitized lung endothelial cells to erastin-induced ferroptosis. Cells with genetic inactivation of either aiPLA_2 or Prdx6-peroxidase were more sensitive to ferroptosis than WT cells, but less sensitive than KO cells. We then conducted RNA-seq analyses in Prdx6-depleted cells to further explore how the loss of Prdx6 sensitizes lung endothelial cells to ferroptosis. Prdx6 KD upregulated transcriptional

[*]Corresponding author. 3040 VLSB MC 3140, Berkeley, CA, 94720, USA. jpv-m@berkeley.edu (J.P. Vázquez-Medina).
[1]Equal contribution.
[2]Current affiliation: Department of Biological Sciences, San Jose State University.

CRediT authorship contribution statement

Julia María Torres-Velarde: Visualization, Methodology, Investigation, Data curation, Conceptualization, Writing – review & editing. **Kaitlin N. Allen:** Data curation, Investigation, Methodology, Writing – review & editing. **Andrea Salvador-Pascual:** Data curation, Formal analysis, Investigation, Methodology, Writing – review & editing. **Roberto G. Leija:** Investigation, Methodology, Writing – review & editing. **Diamond Luong:** Investigation, Methodology, Writing – review & editing. **Diana Daniela Moreno-Santillán:** Conceptualization, Data curation, Investigation, Visualization, Writing – review & editing. **David C. Ensminger:** Writing – review & editing, Visualization, Data curation. **José Pablo Vázquez-Medina:** Writing – review & editing, Writing – original draft, Visualization, Supervision, Project administration, Investigation, Funding acquisition, Formal analysis, Data curation, Conceptualization.

Appendix A. Supplementary data

Supplementary data to this article can be found online at https://doi.org/10.1016/j.freeradbiomed.2024.04.208.

signatures associated with selenoamino acid metabolism and mitochondrial function. Accordingly, Prdx6 deficiency blunted mitochondrial function and increased GPx4 abundance whereas GPx4 KD had the opposite effect on Prdx6. Moreover, we detected Prdx6 and GPx4 interactions in intact cells, suggesting that both enzymes cooperate to suppress lipid peroxidation. Notably, Prdx6-depleted cells remained sensitive to erastin-induced ferroptosis despite the compensatory increase in GPx4. These results show that Prdx6 suppresses ferroptosis in lung endothelial cells and that both aiPLA$_2$ and Prdx6-peroxidase contribute to this effect. These results also show that Prdx6 supports mitochondrial function and modulates several coordinated cytoprotective pathways in the pulmonary endothelium.

Graphical Abstract

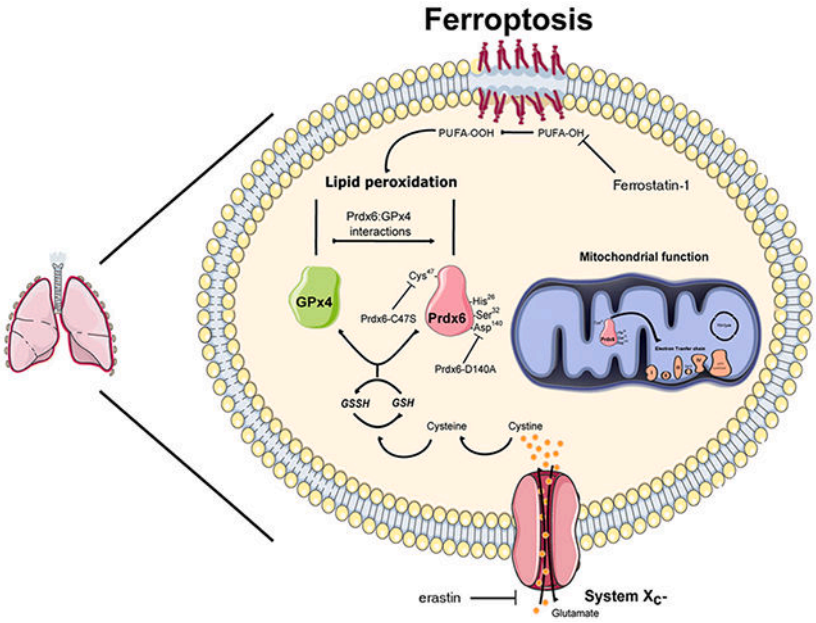

Keywords

Cell death; aiPLA$_2$; Integrated stress response; TP53; 14-3-3ε; GPx4; Mitochondria

1. Introduction

Peroxiredoxin 6 (1-cys peroxiredoxin, Prdx6) is an atypical peroxiredoxin widely expressed throughout the body with the lungs, brain, and testes showing the highest levels [1]. In contrast to other peroxiredoxins, Prdx6 lacks a resolving cysteine and uses glutathione (GSH) to complete its peroxidatic reaction [2–5]. Besides its GSH peroxidase activity, Prdx6 expresses acidic, calcium-independent phospholipase A$_2$ (aiPLA$_2$) [6–8] and lysophosphatidylcholine acyltransferase (Prdx6-LPCAT) activities [9] in separate catalytic sites. The PLA$_2$, LPCAT, and GSH peroxidase activities of Prdx6 are differentially regulated by the subcellular distribution of the protein, substrate binding, and post-translational modifications including hyperoxidation at cysteine 47 and phosphorylation at threonine 177 [10–16].

Prdx6 exhibits maximal PLA_2 activity at acidic pH and maximal GSH peroxidase activity at neutral pH under unstimulated conditions [12]. Hence, when localized to lysosomal-type organelles such as lamellar bodies of type II pneumocytes, Prdx6 functions as a PLA_2 [12]. In contrast, cytosolic Prdx6 functions mainly as a GSH peroxidase [12]. Notably, $aiPLA_2$ increases with enzyme phosphorylation and in the presence of oxidized phospholipid substrate at neutral pH [6]. Moreover, $aiPLA_2$ and the LPCAT activities of Prdx6 appear to represent a two-step coupled reaction without the release of the intermediate lysophosphatidylcholine product [9]. Prdx6 binds to phospholipids with an oxidized fatty acid in the *sn*-2 position at cytosolic pH [6,11,17–19]. Hence, the translocation of Prdx6 to cell membranes under oxidant stress has several biologically relevant effects involving its phospholipid hydroperoxide GSH peroxidase, $aiPLA_2$, and LPCAT activities [9,13,20–22].

Oxidant stress induced by paraquat, hyperoxia or organic peroxides promotes the translocation of Prdx6 to cell membranes [15,19,21–23]. In peroxidized membranes, Prdx6 reduces oxidized phospholipids through its phospholipid hydroperoxide GSH peroxidase activity and replaces the oxidized *sn*-2 fatty acyl group through hydrolysis/reacylation by $aiPLA_2$ and Prdx6-LPCAT [13]. Prdx6 is, therefore, a complete system for the repair of peroxidized cell membranes [13]. Mice and lung cells lacking Prdx6 (Prdx6 KO) or carrying a mutation that prevents Prdx6 from binding to phospholipids (Prdx6-H26A) are unable to repair peroxidized cell membranes after exposure to hyperoxia or treatment with organic peroxides [19–22]. Furthermore, mice with mutations that inactivate either $aiPLA_2$ (Prdx6-D140A) or the GSH peroxidase activity of Prdx6 (Prdx6-C47S) alone show incomplete repair of peroxidized membranes [19–22].

The unique role of Prdx6 as a suppressor of lung lipid peroxidation suggests that this enzyme regulates ferroptosis, and evidence of such effect in cancer cell lines with silenced Prdx6 expression is available [24], although genetic confirmation in cells with full Prdx6 depletion (KO) is still lacking. Similarly, the role of the specific activities of Prdx6 and its relevance in primary cells is unknown. Early work shows that both a PLA_2 and a phospholipid hydroperoxidase activity are necessary to repair peroxidized lipids [25–27]. Ferroptosis is a newly described form of regulated cell death driven by an iron-dependent accumulation of phospholipid hydroperoxides [28–30]. The selenoprotein glutathione peroxidase 4 (GPx4) suppresses ferroptosis through its ability to reduce phospholipid hydroperoxides [31,32]. To date, no other enzymes that regulate the canonical GSH-dependent lipid peroxidation suppression pathway during ferroptosis have been identified [33], but alternative systems that cooperate with GPx4 to suppress the propagation of lipid peroxidation such as FSP1 (ferroptosis suppressor protein 1) and DHODH (dihydroorotate dehydrogenase) are well known [34–36]. Similarly, enzymes that modulate cellular lipid composition including acyl-CoA synthetase long-chain family member 4 (ACSL4) [37–41], lysophosphatidylcholine acyltransferase 3 (LPCAT3) [37,42], and other calcium-independent PLA_2s [43–45] have been shown to regulate ferroptosis.

Here we show that Prdx6 is widely expressed in pulmonary endothelial and epithelial cells and that Prdx6 deletion or knockdown increases erastin-induced, ferrostatin-1-sensitive lipid peroxidation and cell death in murine and human lung endothelial cells in primary culture. Using cells derived from animals harboring single-point mutations that inactivate

either aiPLA$_2$ (Prdx6-D140A) or Prdx6-peroxidase (Prdx6-C47S) we also show that both activities participate in the anti-ferroptotic effect of Prdx6. Moreover, we found that Prdx6 deficiency induces transcriptional signatures associated with mitochondrial function and selenoamino acid metabolism and corroborated that Prdx6 depletion blunts mitochondrial function and upregulates GPx4 expression and abundance, while GPx4 depletion has the opposite effect. Furthermore, using in situ proximity ligation, we found that Prdx6 interacts with GPx4, suggesting that both proteins cooperate to counteract lipid peroxidation. Hence, Prdx6 suppresses ferroptosis by limiting lipid peroxidation through both aiPLA$_2$ and Prdx6-peroxidase and likely by supporting mitochondrial function and modulating other cytoprotective pathways in the pulmonary endothelium.

2. Methods

2.1. Animals

The use of mice for these studies was approved by UC Berkeley's Animal Care and Use Committee (AUP-2022-05-15358). The generation of Prdx6 KO mice is described in Ref. [1]. The generation of Prdx6 KI mice is described in Refs. [21,46]. Prdx6-D140A mice harbor a single amino acid mutation at D140, one of the constituents of the Prdx6-PLA$_2$ catalytic triad. This mutation abolishes the aiPLA$_2$ activity without affecting the peroxidase activity. Prdx6-C47S mice lack peroxidase activity due to a single-point mutation in the catalytic cysteine (C47) but retain aiPLA$_2$ activity. The neomycin resistance cassette that was used in clonal selection during the generation of these mutant mice has been removed using flanking flippase recombinase target (FRT) sites. Unaltered Prdx6 protein levels have been previously confirmed [46]. Prdx6 KO and KI mice were generated by Dr. Aron Fisher (University of Pennsylvania) and obtained through the Mutant Mouse Resource and Research Center (MMRRC).

2.2. Confocal microscopy

Mouse lungs were processed as previously described [46,47]. Lung sections were stained with Prdx6, GPx4 or SLC7A11 antibodies diluted 1:200. GPx4 and SLC7A11 antibodies were obtained commercially (GPx4: Abcam, Cambridge, MA, catalog number: ab125066). The SLC7A11 antibody (Proteintech, Rosemont, IL, catalog number: 26864-1-AP) has been previously validated by over-expression and knockdown (KD) [48,49]. Prdx6 antibodies were a kind gift of Dr. Aron Fisher. Prdx6 antibodies are described in Refs. [10,16] and were previously validated using Prdx6 KO lungs [46]. Sections were incubated with anti-rabbit Alexa 594 secondary antibodies and Alexa 488-CD144 (ve-cadherin, eBioscience catalog number: 53-1441-82) or FITC-CD326 (epCAM, eBioscience catalog number: 14-5791-8) antibodies diluted 1:200. Sections were mounted in VECTASHIELD medium (Vector Laboratories, Burlingame, CA) and imaged using a Zeiss 780 laser-scanning confocal microscope fitted with a 40X objective and Zen software.

2.3. Primary cell isolation and culture

Murine pulmonary microvascular endothelial cells (MPMVECs) were isolated from freshly harvested WT, Prdx6 KO and Prdx6 KI mouse lungs using magnetic beads coated with PECAM-1 antibodies and purified by FACS as previously described [46,47]. MPMVECs

were maintained in DMEM (Gibco, Thermo Fisher Scientific, Waltham, MA) supplemented with FBS (Seradigm, VWR, Radnor, PA), HEPES (Gibco), and Antimycotic/Antibiotic solution (Gibco). Primary human pulmonary microvascular endothelial cells (HPMVECs) isolated from normal lung tissue were obtained from Cell Biologics (Chicago, IL) and maintained in commercial growth media (Cell Biologics, catalog number: H1168).

2.4. Induction and inhibition of ferroptosis

Endothelial monolayers were treated with erastin (BioVison, Milpitas, CA, catalog number: B1502) with or without co-treatment with ferrostatin-1 (Fer-1, BioVison, catalog number: 2230) for 24 h. Erastin-induced GSH depletion was confirmed using a commercial kit (Promega Corporation, Madison, WI, catalog number: V6911) following the manufacturer's recommendations. After treatment, cells were assayed for viability/cytotoxicity, lipid peroxidation, gene expression and protein abundance.

2.5. Measurement of cell death and lipid peroxidation

Cell viability and cytotoxicity were measured using a commercial imaging kit (Thermo Fisher, catalog number: R37601). Cells plated in glass-bottom dishes were treated with drugs as described above. Staining and Hoechst solutions were added during the last 30 min of the treatment. In separate experiments, lipid peroxidation was detected using live-cell microscopy in cells loaded with Liperfluo (10 μM, Dojindo, Rockville, MD, catalog number: L248-10) during the last hour of the drug incubation period. Cells were imaged using a fluorescence microscope (Zeiss Axio Observer) fitted with a 20X objective and Zen software (Zeiss, Thornwood, NY, USA). Fluorescence intensity was quantified using ImageJ.

2.6. Extracellular flux assays

Cells seeded in Seahorse plates (Agilent, Santa Clara, CA) were washed with Seahorse assay medium supplemented with 5.56 mM glucose, 1 mM pyruvate, and 4 mM L-glutamine, and placed in a CO_2-free incubator for 1 h. Oxygen consumption rates (OCR) were measured in a calibrated extracellular flux analyzer (Agilent) in the presence of oligomycin (1 μM), carbonyl cyanide-p-trifluoromethoxyphenylhydrazone (FCCP, 1 or 2 μM for human or mouse cells respectively), and rotenone/antimycin A (0.5 μM). OCR values were normalized to total protein measured with a Qubit fluorometer (Invitrogen, Carlsbad, CA). Mitochondrial function was calculated according to Ref. [50].

2.7. In situ proximity ligation

Visualization of protein-protein interactions in intact cells was conducted using Duolink II in situ proximity ligation kits (Olink, Uppsala, Sweden) with mouse anti-Prdx6 (EMD Millipore, Burlington, MA, catalog number: MABN1797) and rabbit anti-GPx4 antibodies (Abcam, Cambridge, MA, catalog number: ab125066) following the procedure described previously [46,47]. Nonspecific mouse and rabbit IgGs were used as negative controls. Cells were fixed with 1:1 ice-cold methanol/acetone, washed, permeabilized, treated with blocking reagent for 1 h, and incubated overnight with primary antibodies diluted 1:100. The Duolink II kit contains secondary antibodies to rabbit and mouse IgG, each attached

to a unique synthetic oligonucleotide; if the 2 proteins are in proximity, ligation causes the 2 oligonucleotides to hybridize, allowing DNA replication and amplification of a red fluorescent signal [51,52]. The resulting signal was imaged with a fluorescence microscope (Zeiss Axio Observer) fitted with a 63X objective and Zen software.

2.8. RT-qPCR

Total RNA was extracted using Trizol (Invitrogen catalog number: 15596026). Genomic DNA contamination was removed using a Turbo DNA-free kit (Thermo Fisher catalog number: AM1907) and confirmed by lack of amplification using RT-PCR. RNA was quantified with a Qubit fluorometer (Invitrogen). cDNA was synthesized using a High-Capacity cDNA Reverse Transcription kit (Invitrogen catalog number: 4368814). RT-qPCR was performed with DyNAmo Flash SYBR Green master mix (Thermo Fisher catalog number: F415L) under the following conditions: 7 min at 95 °C, followed by 40 cycles of 20 s at 95 °C, and 30 s at 60 °C. Relative expression was calculated using the comparative $2^{-\Delta\Delta CT}$ method with the geometric mean of *gapdh* and *18s* as house-keeping genes [53]. Primer sequences are listed in Table S1.

2.9. Gene knockdown

HPMVECs were transfected with Prdx6 siRNAs (Ambion, Austin, TX, catalog number: 4390826, s18429), GPx4 siRNAs (Ambion, catalog number: 4392429, s6112) or scrambled non-targeting (NT) control siRNA sequences (Ambion, catalog number: 4390844) using Lipofectamine iRNAMAX (Invitrogen, catalog number: 13778150). Gene knockdown (KD) was confirmed by RT-qPCR and Western blot.

2.10. RNA-seq and transcriptome analyses

RNA integrity was measured with an Agilent 2100 Bioanalyzer (Agilent Technologies, Santa Clara, CA). cDNA libraries were prepared from poly(A)-captured mRNA and sequenced to a total of 20 million reads per sample on an Illumina platform (Illumina, San Diego, CA). Reads were mapped to the human genome using STAR aligner. Transcript levels were quantified using RSEM. Genes differentially expressed (DE) between cells transfected with NT and Prdx6 siRNAs, with and without erastin treatment were identified at an FDR of 5% using DESeq2. Reactome pathways and gene ontology (GO) terms enriched among DE genes were identified using Gene Set Enrichment Analysis (GSEA) [54]. Functional interaction networks (FIN) and enrichment analyses were built from enriched Reactome and KEGG pathways using Cytoscape [55,56] and WebGestalt [57]. *Cis*-regulatory analysis was performed using iRegulon in Cytoscape at an FDR of 5% [58].

2.11. Immunoblotting

Western blot was conducted as previously described [46]. Primary antibodies were used at the following dilutions: Prdx6 [10,16] 1:1,500, GPx4 (Abcam, Cambridge, MA, catalog number: ab125066) 1:3000. Membranes were incubated with IRDye 800CW secondary antibodies (LI-COR Biosciences, Lincoln, NE) and imaged using a two-color NIR system (Azure c500, Azure Biosystems, Dublin, CA). Blots were stripped and re-probed with GAPDH antibodies (Cell Signaling Technologies, Danvers, MA, catalog number: 2118)

diluted 1:2000. Individual bands were quantified using ImageJ and normalized to GAPDH levels.

2.12. Statistical analyses

Normality and equal variance were evaluated using Shapiro-Wilk and Levene tests. Differences among groups were determined using t-tests or ANOVAs with Tukey's post-hoc correction and considered significant when $p < 0.05$. Statistical analyses were conducted using GraphPad Prism v9. Data are presented as mean ± SD of at least three independent experiments.

3. Results

3.1. Prdx6 is a widely expressed lung phospholipid hydroperoxidase

We compared whole lung mRNA levels of Prdx6 and GPx4. Prdx6 expression was five times higher than GPx4 expression (Fig. 1A). We then visualized the spatial localization of Prdx6 and GPx4 in the lung. Prdx6 and GPx4 were expressed in both pulmonary endothelial (Vecadherin$^+$) and epithelial (epCAM$^+$) cells (Fig. 1B). Our previous work shows that Prdx6 deletion reduces lung phospholipid hydroperoxide GSH peroxidase activity by 4.5-fold [46] and that Prdx6 KO animals exhibit impaired lung lipid peroxidation repair [20]. Similarly, early work shows that Prdx6 KO animals exhibit decreased survival rates and more severe lung injury than WT animals exposed to hyperoxia or paraquat [59,60], whereas transgenic animals overexpressing Prdx6 show increased resistance to lung injury in hyperoxia [61]. Together, these data suggest that Prdx6 is important to limit lipid peroxidation in the lung.

3.2. Prdx6 suppresses erastin-induced ferroptosis in lung endothelial cells

We studied the effects of erastin on lipid peroxidation and cell death in MPMVECs. Erastin inhibits the system xc$^-$ cystine/glutamate antiporter subsequently decreasing intracellular GSH [62]. Both, Prdx6 and GPx4 use GSH to reduce phospholipid hydroperoxides [18,31,63]. System xc$^-$ is notoriously over-expressed in cancer cells [64], but previous reports show that it also mediates cystine uptake in cultured human umbilical vein endothelial cells [65], although the in vivo significance of system xc$^-$ in the pulmonary endothelium is unknown. Hence, we first tested whether system xc$^-$ is expressed in the lung endothelium in vivo. Using confocal microscopy, we found that the SLC7A11 subunit of system xc$^-$ colocalizes with vascular endothelial cadherin in the lungs of healthy mice (Fig. 2A). We then corroborated that erastin treatment depletes GSH levels in MPMVECs in primary culture (Fig. 2B). Consistent with this observation, erastin increased lipid peroxidation by 12-fold (Fig. 2C); this increase was prevented by co-treatment with the synthetic antioxidant/ferroptosis inhibitor Fer-1 [66] (Fig. 2C). Erastin-induced lipid peroxidation was higher in MPMVECs isolated from Prdx6 KO mice than in cells isolated from WT mice (Fig. 2C). Similar to WT cells, Fer-1 prevented erastin-induced lipid peroxidation in Prdx6 KO cells (Fig. 2C). These results show that Prdx6 suppresses erastin-induced lipid peroxidation in MPMVECs. Therefore, we then tested whether loss of Prdx6 sensitizes MPMVECs to erastin-induced ferroptosis. Erastin induced cell death in a dose-dependent manner in WT cells ($F = 109.4$, $p < 0.0001$, Fig. 2D). Erastin-induced cell death was 2.6-fold higher at the 1 μM dose ($p_{adjust} < 0.0001$) and 1-fold higher at the 5 μM

dose (p_{adjust} = 0.0059) in Prdx6 KO compared to WT cells (Fig. 2D). Erastin-induced cell death was prevented by treatment with Fer-1 in both WT and Prdx6 KO cells. These results show that Prdx6 suppresses erastin-induced ferroptosis in MPMVECs.

We next tested the individual contributions of aiPLA$_2$ and Prdx6-peroxidase to the anti-ferroptotic effect of Prdx6 using MPMVECs isolated from Prdx6-KI mice with single point mutations that inactivate each of those Prdx6 activities alone. Similar to WT and Prdx6 KO cells, Fer-1 suppressed ferroptosis in Prdx6-KI cells (Fig. 2D). Both Prdx6-D140A and Prdx6-C47S cells were more sensitive to erastin than WT cells, but less sensitive than Prdx6 KO cells at the 1 μM dose, whereas no significant differences were observed between WT and Prdx6-KI cells at the 5 μM dose (Fig. 2D). These results show that both the PLA$_2$ and peroxidase activities of Prdx6 contribute to the anti-ferroptotic effect of Prdx6.

We silenced Prdx6 expression in primary HPMVECs to test whether the effects observed in murine cells translate to human cells. Prdx6 KD with siRNAs decreased Prdx6 mRNA levels by 99% ($t = 29.81$, $p < 0.0001$) and Prdx6 protein abundance by 85% ($t = 13.55$, $p = 0.0002$, Fig. 2E). Prdx6 KD in HPMVECs increased cell death with (p_{adjust} = 0.0016) and without (p_{adjust} = 0.0005) erastin treatment (Fig. 2F). These results show that Prdx6 deficiency sensitizes primary murine and human lung endothelial cells to ferroptosis.

3.3. Prdx6-deficient cells upregulate transcriptional signatures of selenoamino acid metabolism, mitochondrial function and cellular stress

We further explored how Prdx6 deficiency sensitizes cells to ferroptosis by conducting RNA-seq in HPMVECs with Prdx6 KD with and without erastin treatment (Fig. 3A–C). Top differentially expressed (DE) genes in Prdx6 KD cells include known regulators of iron metabolism and ferroptosis such as *hmox1* [67,68], *cybrd1* [69,70], and *sfxn1* [71,72] (Fig. 3B). *Hmox1* was also the top DE gene in cells treated with erastin but transfected with NT siRNAs (Fig. 3A), and one of the top genes in Prdx6 KD cells treated with erastin (Fig. 3C). Consistent with this observation, previous work shows that Prdx6 KD upregulates *hmox1* [24], that *hmox1* overexpression exacerbates ferroptosis and that *hmox1* KD or inhibition attenuates ferroptosis in several cancer cell lines and vascular endothelial cells [68,73].

We then identified Reactome pathways enriched in cells transfected with NT siRNAs and treated with erastin (Fig. 3D), and in cells with Prdx6 KD (Fig. 3E). Upregulated pathways enriched in cells transfected with NT siRNAs and treated with erastin include ER stress, cellular response to stress and response to heme deficiency while extracellular matrix degradation was downregulated (Fig. 3D). Top upregulated pathways in untreated cells with Prdx6 KD include selenoamino acid metabolism, selenocysteine synthesis, cellular respiration and DNA damage (Fig. 3E), while relevant gene ontology (GO) terms include extracellular matrix organization, biological oxidations, phospholipid translocation, endothelial cell morphogenesis and transcription regulation in response to iron (Fig. 3H).

We constructed functional interaction networks (FIN) [56] using Reactome and KEGG pathways enriched in cells with Prdx6 KD (Fig. S1A). We identified seven network modules in the FIN. Modules 0 and 2 grouped genes related to cell cycle; module 1 grouped genes involved in translation, response to amino acid deficiency, and selenoamino

acid metabolism, whereas modules 3, 4, 5, and 7 grouped genes involved in oxidative phosphorylation, mitochondrial protein import, TCA cycle and respiratory electron transport. Module 6 was associated with changes in extracellular organization (Fig. S1A). *Cis*-regulatory analysis [58] identified ETV6 (ETS Variant Transcription Factor 6), ZBTB33 (transcriptional regulator Kaiso) and TP53 (cellular tumor antigen p53) as the most enriched transcription factors (TF) in promoters of genes DE in untreated cells with Prdx6 KD (Fig. 3G–S1B). These TFs are crucial for endothelial cell development [74,75], transcriptional regulation [76–81], cell cycle arrest [82], oxidative stress and cell death [83,84]. Moreover, TP53 delays the onset of ferroptosis by promoting intracellular GSH conservation [85]. In cells transfected with NT siRNAs and treated with erastin (Fig. 3F), the main TF identified in our analyses were CEBPB, which regulates TP53 and possibly GPx4 and FSP1 [86–88], ATF3, which promotes ferroptosis by suppressing system xc^- [89], and IRF9, which has been previously linked to ferroptosis [90]. Together, our results show that Prdx6 deficiency alters transcriptional signatures associated with mitochondrial function, selenoamino acid metabolism and cellular stress in addition to increasing susceptibility to lipid peroxidation. Hence, Prdx6 regulates ferroptosis by suppressing lipid peroxidation and likely by modulating other cytoprotective pathways.

To further explore the effects of Prdx6 deficiency on ferroptosis, we identified genes differentially expressed (DE) in Prdx6 KD cells treated with erastin but not DE in untreated Prdx6 KD cells or cells transfected with NT siRNAs and treated with erastin (Fig. 3I). Differential expression of *gpx3, gpx7, g6pd, txndc12, txnrd2, nqo1*, and *sod2* suggests that Prdx6 deficiency influences the expression of other antioxidant genes during ferroptosis. Similarly, differential expression of several genes involved in lipid metabolism including *pla2g7, pnpla2, pld6, atg3, c12orf49*, and *zdhhc18*, underscores the role of $aiPLA_2$ in the response to ferroptosis in lung endothelial cells. Additionally, differential expression of *cdc20, chek1, bub1b, cdk2, mcm4, ccne1*, and*pkmyt1* suggests that Prdx6 plays a role in cell cycle regulation during ferroptosis, which coincides with cell cycle arrest [91]. Finally, differential expression of *tnfaip1, tnfaip2, tlr6, il15, smad1, cxcl2, cercam, nfkb2, ifngr2* and *if16* suggests that Prdx6 modulates inflammatory pathways during ferroptosis. Consistent with this observation, GSEA analyses for Reactome and KEEG pathways in genes DE only in Prdx6 KD cells treated with erastin showed enrichment for MAPK signaling and de-enrichment for cell cycle and cytokine and chemokine signaling (Table S2).

3.4. Prdx6 deficiency increases GPx4 expression and abundance while suppressing mitochondrial function

Our RNA-seq analyses show that Prdx6 KD upregulates transcriptional signatures associated with selenocysteine synthesis, selenoamino acid metabolism and mitochondrial function (Fig. 3E–S1A). Hence, we functionally tested whether Prdx6 expression influences mitochondrial function and abundance of the selenoprotein GPx4. Previous analyses of co-essentiality show a positive association between GPx4 and Prdx6, suggesting functional links between these two proteins [92]. Similarly, functional analyses using the $aiPLA_2$ inhibitor MJ33 and the GPx4 inhibitor ML210 suggest that both activities cooperate to repair oxidized phospholipids [93]. Hence, we used situ proximity ligation to test whether Prdx6 interacts with GPx4 in intact cells. We found spatial associations of Prdx6 and

GPx4 (Fig. 4A), suggesting that both enzymes cooperate to repair lipid peroxidation in pulmonary endothelial cells. When then silenced Prdx6 and measured GPx4 expression and abundance. Prdx6 KD promoted a compensatory increase in GPx4 expression ($t = 2.991$, $p = 0.0403$, Fig. 4B) and protein abundance ($t = 3.795$, $p = 0.0192$, Fig. 4C). To test whether this compensatory effect occurs in GPx4-depleted cells, we silenced GPx4 expression and measured Prdx6 abundance. GPx4 KD with siRNAs decreased GPx4 abundance by 93% ($t = 16.65$, $p < 0.0001$, Fig. 4D). Notably, no apparent decrease in cellular viability was observed in GPx4-depleted cells under basal conditions or upon treatment with 1 μM erastin; however, viability was 21% lower in GPx4 KD cells treated 5 μM erastin than in cells transfected with NT siRNAs ($p = 0.07$; Fig. S2). GPx4 KD increased Prdx6 abundance by 67% ($t = 2.809$, $p = 0.0403$, Fig. 4D). Together, these data show that Prdx6 and GPx4 interact in intact lung endothelial cells and that these cells compensate for the lack of Prdx6 by upregulating GPx4 and vice versa. Remarkably, despite compensatory increases in GPx4, Prdx6-deficient pulmonary endothelial cells remained sensitized to ferroptosis compared WT, Prdx6-KI, or NT-transfected cells (Fig. 2D and F).

Mitochondria seem to play a role in ferroptosis [36,94], and Prdx6 deletion in HepG2 cells induces mitochondrial dysfunction [95]. Consistent with this observation, our RNA-seq data show strong signatures of mitochondrial metabolism in cells with Prdx6 KD (Fig. 3E–S1A). Hence, we conducted metabolic flux assays in Prdx6-deficient murine and human lung endothelial cells to test whether Prdx6 regulates mitochondrial function in this system. Maximal respiration ($p = 0.0005$), and spare respiratory capacity ($p = 0.0286$) were lower in Prdx6 KO compared to WT MPMVECs (Fig. 4E). Similarly, Prdx6 KD in HPMVECs blunted mitochondrial function (Fig. S3). These results show that Prdx6 supports mitochondrial function in lung endothelial cells. Furthermore, these results suggest that dysregulated mitochondrial metabolism in Prdx6-deficient cells may contribute to ferroptosis sensitization.

4. Discussion

Excessive levels of phospholipid hydroperoxides distinguish ferroptosis from other types of cell death [29]. Early work shows that both a PLA_2 and a phospholipid hydroperoxidase activity are necessary to repair peroxidized phospholipids [25–27]. GPx4 suppresses ferroptosis by reducing phospholipid hydroperoxides [32,96] while other proteins such as FSP1 cooperate with GPx4 to prevent lipid peroxidation [34,35]. Notably, GPx4 deficiency in endothelial cells has minimal effects in the presence of low vitamin E [97], suggesting that alternative antioxidant systems regulate lipid peroxidation in these and possibly other cell types [98]. In our previous work, we found that Prdx6 deletion decreases lung phospholipid hydroperoxide GSH peroxidase activity by 4.5-fold [46] whereas mice null for Prdx6 (Prdx6-KO) or with a mutation that prevents Prdx6 from biding phospholipids (Prdx6-H26A) are unable to repair lung lipid peroxidation [20]. Here we found that Prdx6 is widely abundant within the lung, that Prdx6 deficiency sensitizes murine and human lung endothelial cells to ferroptosis and that both the peroxidase and $aiPLA_2$ activities of Prdx6 are important for this effect. Finally, we found that Prdx6 deficiency dysregulates mitochondrial function and upregulates transcriptional signatures of cellular stress and selenoamino acid metabolism, that Prdx6 interacts with GPx4, and that Prdx6 deficiency

results in GPx4 upregulation and vice versa. Therefore, our results show that Prdx6 is a crucial cytoprotective protein that suppresses ferroptosis in the pulmonary endothelium.

Prdx6 expresses PLA_2 activity [6–8,17,99] in addition to its phospholipid hydroperoxide GSH peroxidase activity [18,20]. Both, a PLA_2 and a phospholipid hydroperoxidase activity are required to repair peroxidized phospholipids [25–27]. Prdx6 KO MPMVECs show increased lethality to treatment with organic peroxides compared to WT cells [22]. Overexpression of Prdx6 in KO cells rescues this phenotype whereas expression of mutant Prdx6 with either peroxidase or $aiPLA_2$ alone shows a partial effect [22]. Similarly, lungs from Prdx6 KI mice carrying single point mutations that inactivate either activity alone [100] show incomplete lipid peroxidation repair after treatment with organic peroxides [21]. Thus, both the peroxidase and $aiPLA_2$ activities of Prdx6 are necessary to suppress lipid peroxidation in the lung. Consistent with these observations, here we show that pulmonary endothelial cells derived from KI mice lacking either $aiPLA_2$ or Prdx6-peroxidase alone are more sensitive to ferroptosis than cells derived from WT mice but less sensitive than cells derived from full Prdx6 KO mice, further suggesting that both activities are important for the anti-ferroptotic effect of Prdx6.

The calcium independent PLA_2 enzyme $iPLA_2\beta$ protects against ferroptosis [43,44,101]. Similarly, treatment of non-small cell lung cancer cells (H1299) with an $aiPLA_2$ inhibitor (MJ33) ameliorates ferroptosis [24], suggesting that the PLA_2 activity of Prdx6 ($aiPLA_2$) is critical to suppress ferroptosis in the lung and possibly other tissues [102,103]. CRISPR screens identified Prdx6 as one of the top-scoring genes in Jurkat cells treated with erastin but not in cells treated with RSL3 [72]. RSL3 induces ferroptosis by inhibiting GPx4 [32,104]. Recent evidence shows that the inhibitory effect of RSL3 on GPx4 requires the adaptor protein 14-3-3ε [105], which is also needed for the intracellular trafficking of Prdx6 [106–108]. Hence, it is possible that inhibition of GPx4 with RSL3 also targets Prdx6. Notably, recent analyses of essentiality scores of gene knockouts across one thousand cancer cell lines suggest that Prdx6 and GPx4 might be functionally linked [92,109]. Similarly, functional analyses using MJ33 and the GPx4 inhibitor ML210 show that both activities are necessary to repair peroxidized phospholipids at least in in 3T3-L1 adipocytes [93]. Here, we found that GPx4 and Prdx6 interact in intact cells, further suggesting that both enzymes cooperate to suppress lipid peroxidation. Although the specific structural mechanism driving the interaction of Prdx6 with GPx4 remains to be studied, it is known that Prdx6 dimerizes with glutathione S-transferase via disulfide bonds and that this interaction is necessary for its peroxidase activity [4,5,110]. Hence, it is likely that Prdx6 and GPx4 cooperate to repair peroxidized membranes, which could explain why lung endothelial cells deficient in Prdx6 compensate by upregulating GPx4 and vice versa.

Our RNA-seq data show enrichment for selenoamino metabolism and selenocysteine synthesis in cells with depleted Prdx6 expression and our silencing experiments corroborate that cells with Prdx6 KD increase expression of the selenoprotein GPx4. Furthermore, our in situ proximity ligation results suggest that Prdx6 and GPx4 might be functionally linked. Consistent with this observation, co-essentiality analyses show that Prdx6 is part of the selenocysteine gene cluster, even though Prdx6 does not contain selenocysteine, further suggesting a potential functional link between Prdx6 and GPx4 [92,109,111].

A second possibility is that Prdx6 participates in selenoprotein biosynthesis by forming selenyl sulfides with selenocysteine, effectively serving as a selenide carrier given its strong associations with selenocysteine lyase and selenophosphate synthetase 2 [92], although further experimental analyses are required to test this idea.

Besides its established role in regulating lipid peroxidation, Prdx6 may also help sustain mitochondrial function [112,113]. Prdx6 KO mice show increased hepatic mitochondrial dysfunction compared to WT controls after ischemia/reperfusion injury [114]. Similarly, Prdx6 KO in hepatocarcinoma cells decreases oxygen consumption and alters mitochondrial morphology [95]. Our results show that Prdx6 deficiency induces mitochondrial dysfunction in lung endothelial cells, but it is still unclear if this effect increases sensitivity to ferroptosis. Mitochondrial GSH is necessary for proliferation [115] and the role of a mitochondrial phospholipid hydroperoxide GSH peroxidase activity in the suppression of cell death has been known for over two decades [116,117]. Recent studies confirm a pivotal role of mitochondria in the onset of ferroptosis [36,94,118–121]. Prdx6 is a constituent of the mitochondrial proteome [122], but its role in the removal of mitochondrial phospholipid hydroperoxides remains underexplored.

Our results show enrichment for ATF4-mediated ER stress and inflammatory signaling in HPMVECs treated with erastin, suggesting that these pathways are an important component of the transcriptional response to erastin-induced ferroptosis in vascular endothelial cells. Mitochondrial dysfunction triggers the integrated stress response, which induces ATF4 [123,124]. Pharmacological inhibition of system xc^-, which is regulated by ATF4 [125], also promotes ER stress [62]. In our experiments, we found that ATF3 is one of the main TFs involved in the transcriptional response to erastin treatment in lung endothelial cells. ATF3 promotes ferroptosis by increasing intracellular iron and stimulating hydrogen peroxide production while suppressing system xc^- expression [89,126]. CEBPB and IRF9, the other two main TFs identified in our analysis, modulate inflammatory pathways and are involved in pyroptosis [127–130]. The link between ferroptosis and pyroptosis is poorly understood but an active area of research [131–133]. Prdx6 is a major player in the inflammatory response of the pulmonary endothelium [134]. Thus, it is possible that in addition to increasing susceptibility to ferroptosis, Prdx6 deficiency sensitizes lung endothelial cells to other cell modalities. Moreover, identification of ETV6, ZBTB33, and TP53 as the main TFs mediating the transcriptional response to Prdx6 deficiency in untreated cells further suggests that Prdx6 modulates cell cycle progression, which also sensitizes cells to ferroptosis [91].

5. Conclusions

In summary, we found that Prdx6 modulates ferroptosis in lung endothelial cells by suppressing lipid peroxidation, and that both aiPLA$_2$ and the peroxidase activity of Prdx6 are necessary for this effect. We also found that Prdx6 interacts with GPx4, suggesting that both proteins cooperate to suppress lipid peroxidation. Moreover, we found that Prdx6 deficiency increases GPx4 abundance but impairs mitochondrial function and is associated with transcriptional signatures of selenoamino acid metabolism, cellular stress and inflammation. Thus, Prdx6 protects lung endothelial cells against ferroptosis by modulating several coordinated mechanisms.

Supplementary Material

Refer to Web version on PubMed Central for supplementary material.

Acknowledgments

We thank Dr. Aron Fisher (University of Pennsylvania) for providing custom-made Prdx6 antibodies and for sharing Prdx6 KO and KI mice through MMRRC. Confocal imaging was conducted at the UC Berkeley CRL Molecular Imaging Center, supported by NSF DBI-1041078. JMT-V was supported by a UC MEXUS-CONACyT postdoctoral fellowship. KNA was supported by an NSF GRFP. David Ensminger was supported by an NSF PRFB. This research was funded by NIGMS R35GM146951. Early versions of this work were presented at the 2019, 2020, and 2022 Annual Meetings of the Society for Redox Biology and Medicine.

Declaration of competing interest

The authors declare the following financial interests/personal relationships which may be considered as potential competing interests: Jose Pablo Vazquez-Medina reports financial support was provided by National Institute of General Medical Sciences. Jose Pablo Vazquez-Medina reports a relationship with National Institute of General Medical Sciences that includes: funding grants. If there are other authors, they declare that they have no known competing financial interests or personal relationships that could have appeared to influence the work reported in this paper.

References

[1]. Mo Y, et al. , 1-Cys peroxiredoxin knock-out mice express mRNA but not protein for a highly related intronless gene, FEBS Lett. 555 (2) (2003) 192–198. [PubMed: 14644414]

[2]. Kang SW, Baines IC, Rhee SG, Characterization of a mammalian peroxiredoxin that contains one conserved cysteine, J. Biol. Chem 273 (11) (1998) 6303–6311. [PubMed: 9497358]

[3]. Manevich Y, Feinstein S, Fisher A, Activation of the antioxidant enzyme 1-CYS peroxiredoxin requires glutathionylation mediated by heterodimerization with πGST, Proc. Natl. Acad. Sci. USA 101 (11) (2004) 3780–3785. [PubMed: 15004285]

[4]. Zhou S, et al. , Functional interaction of glutathione S-transferase pi and peroxiredoxin 6 in intact cells, Int. J. Biochem. Cell Biol 45 (2) (2013) 401–407. [PubMed: 23164639]

[5]. Zhou S, et al. , Peroxiredoxin 6 homodimerization and heterodimerization with glutathione S-transferase pi are required for its peroxidase but not phospholipase A2 activity, Free Radic. Biol. Med 94 (2016) 145–156. [PubMed: 26891882]

[6]. Fisher AB, The phospholipase A(2) activity of peroxiredoxin 6, J. Lipid Res 59(7) (2018) 1132–1147. [PubMed: 29716959]

[7]. Kim T-S, et al. , Cloning and expression of rat lung acidic Ca2+-independent PLA2 and its organ distribution, Am. J. Physiol. Lung Cell Mol. Physiol 274 (5) (1998) L750–L761.

[8]. Kim T-S, et al. , Identification of a human cDNA clone for lysosomal type Ca2+-independent phospholipase A2 and properties of the expressed protein, J. Biol. Chem 272 (4) (1997) 2542–2550. [PubMed: 8999971]

[9]. Fisher AB, et al. , A novel lysophosphatidylcholine acyl transferase activity is expressed by peroxiredoxin 6, J. Lipid Res 57 (4) (2016) 587–596. [PubMed: 26830860]

[10]. Chatterjee S, et al. , Peroxiredoxin 6 phosphorylation and subsequent phospholipase A2 activity are required for agonist-mediated activation of NADPH oxidase in mouse pulmonary microvascular endothelium and alveolar macrophages, J. Biol. Chem 286 (13) (2011) 11696–11706. [PubMed: 21262967]

[11]. Chen J-W, et al. , 1-Cys peroxiredoxin, a bifunctional enzyme with glutathione peroxidase and phospholipase A2 activities, J. Biol. Chem 275 (37) (2000) 28421–28427. [PubMed: 10893423]

[12]. Fisher AB, Peroxiredoxin 6: a bifunctional enzyme with glutathione peroxidase and phospholipase A_2 activities, Antioxidants Redox Signal. 15 (3) (2011) 831–844.

[13]. Fisher AB, Peroxiredoxin 6 in the repair of peroxidized cell membranes and cell signaling, Arch. Biochem. Biophys 617 (2017) 68–83. [PubMed: 27932289]

[14]. Kim SY, et al. , H2O2-dependent hyperoxidation of peroxiredoxin 6 (Prdx6) plays a role in cellular toxicity via up-regulation of iPLA2 activity, J. Biol. Chem 283 (48) (2008) 33563–33568. [PubMed: 18826942]

[15]. Manevich Y, Fisher AB, Peroxiredoxin 6, a 1-Cys peroxiredoxin, functions in antioxidant defense and lung phospholipid metabolism, Free Radic. Biol. Med 38 (11) (2005) 1422–1432. [PubMed: 15890616]

[16]. Wu Y, et al. , Mitogen-activated protein kinase-mediated phosphorylation of peroxiredoxin 6 regulates its phospholipase A2 activity, Biochem. J 419 (3) (2009) 669–679. [PubMed: 19140803]

[17]. Fisher AB, et al. , A competitive inhibitor of phospholipase A2 decreases surfactant phosphatidylcholine degradation by the rat lung, Biochem. J 288 (2) (1992) 407–411. [PubMed: 1463444]

[18]. Fisher AB, et al. , Phospholipid hydroperoxides are substrates for non-selenium glutathione peroxidase, J. Biol. Chem 274 (30) (1999) 21326–21334. [PubMed: 10409692]

[19]. Manevich Y, et al. , Binding of peroxiredoxin 6 to substrate determines differential phospholipid hydroperoxide peroxidase and phospholipase A2 activities, Arch. Biochem. Biophys 485 (2) (2009) 139–149. [PubMed: 19236840]

[20]. Fisher AB, et al. , Peroxiredoxin 6 phospholipid hydroperoxidase activity in the repair of peroxidized cell membranes, Redox Biol. 14 (2018) 41–46. [PubMed: 28865296]

[21]. Li H, et al. , Critical role of peroxiredoxin 6 in the repair of peroxidized cell membranes following oxidative stress, Free Radic. Biol. Med 87 (2015) 356–365. [PubMed: 26117327]

[22]. Lien Y-C, et al. , The roles of peroxidase and phospholipase A2 activities of peroxiredoxin 6 in protecting pulmonary microvascular endothelial cells against peroxidative stress, Antioxidants Redox Signal. 16 (5) (2012) 440–451.

[23]. Liu G, et al. , Comparison of glutathione peroxidase 1 and peroxiredoxin 6 in protection against oxidative stress in the mouse lung, Free Radic. Biol. Med 49 (7) (2010) 1172–1181. [PubMed: 20627125]

[24]. Lu B, et al. , Identification of PRDX6 as a regulator of ferroptosis, Acta Pharmacol. Sin 40 (10) (2019) 1334–1342. [PubMed: 31036877]

[25]. Sevanian A, Muakkassah-Kelly SF, Montestruque S, The influence of phospholipase A2 and glutathione peroxidase on the elimination of membrane lipid peroxides, Arch. Biochem. Biophys 223 (2) (1983) 441–452. [PubMed: 6859870]

[26]. Girotti AW, Lipid hydroperoxide generation, turnover, and effector action in biological systems, J. Lipid Res 39 (8) (1998) 1529–1542. [PubMed: 9717713]

[27]. van Kuijk FJ, et al. , A new role for phospholipase A2: protection of membranes from lipid peroxidation damage, Trends Biochem. Sci 12 (1987) 31–34.

[28]. Dixon SJ, et al. , Ferroptosis: an iron-dependent form of nonapoptotic cell death, Cell 149 (5) 2012 1060–1072. [PubMed: 22632970]

[29]. Wiernicki B, et al. , Excessive phospholipid peroxidation distinguishes ferroptosis from other cell death modes including pyroptosis, Cell Death Dis. 11 (10) (2020) 1–11. [PubMed: 31911576]

[30]. Yang WS, Stockwell BR, Ferroptosis: death by lipid peroxidation, Trends Cell Biol. 26 (3) (2016) 165–176. [PubMed: 26653790]

[31]. Ursini F, et al. , Purification from pig liver of a protein which protects liposomes and biomembranes from peroxidative degradation and exhibits glutathione peroxidase activity on phosphatidylcholine hydroperoxides, Biochim. Biophys. Acta Lipids Lipid. Metabol 710 (2) 1982) 197–211.

[32]. Yang WS, et al. , Regulation of ferroptotic cancer cell death by GPX4, Cell 156 (1–2) (2014) 317–331. [PubMed: 24439385]

[33]. Ursini F, Maiorino M, Lipid peroxidation and ferroptosis: the role of GSH and GPx4, Free Radic. Biol. Med 152 (2020) 175–185. [PubMed: 32165281]

[34]. Bersuker K, et al. , The CoQ oxidoreductase FSP1 acts parallel to GPX4 to inhibit ferroptosis, Nature 575 (7784) (2019) 688–692. [PubMed: 31634900]

[35]. Doll S, et al. , FSP1 is a glutathione-independent ferroptosis suppressor, Nature 575 (7784) (2019) 693–698. [PubMed: 31634899]

[36]. Mao C, et al. , DHODH-mediated ferroptosis defence is a targetable vulnerability in cancer, Nature 593 (7860) (2021) 586–590. [PubMed: 33981038]

[37]. Doll S, et al. , ACSL4 dictates ferroptosis sensitivity by shaping cellular lipid composition, Nat. Chem. Biol 13 (1) (2017) 91–98. [PubMed: 27842070]

[38]. Xu Y, et al. , Inhibition of ACSL4 attenuates ferroptotic damage after pulmonary ischemia-reperfusion, Faseb. J 34 (12) (2020) 16262–16275. [PubMed: 33070393]

[39]. Li Y, et al. , Ischemia-induced ACSL4 activation contributes to ferroptosis-mediated tissue injury in intestinal ischemia/reperfusion, Cell Death Differ. 26 (11) (2019) 2284–2299. [PubMed: 30737476]

[40]. Zhang H-L, et al. , PKCβII phosphorylates ACSL4 to amplify lipid peroxidation to induce ferroptosis, Nat. Cell Biol (2022) 1–11.

[41]. Xiao F-J, et al. , miRNA-17-92 protects endothelial cells from erastin-induced ferroptosis through targeting the A20-ACSL4 axis, Biochem. Biophys. Res. Commun 515 (3) (2019) 448–454. [PubMed: 31160087]

[42]. Dixon SJ, et al. , Human haploid cell genetics reveals roles for lipid metabolism genes in nonapoptotic cell death, ACS Chem. Biol 10 (7) (2015) 1604–1609.

[43]. Beharier O, et al. , PLA2G6 guards placental trophoblasts against ferroptotic injury, Proc. Natl. Acad. Sci. USA 117 (44) (2020) 27319–27328. [PubMed: 33087576]

[44]. Sun W-Y, et al. , Phospholipase iPLA 2 β averts ferroptosis by eliminating a redox lipid death signal, Nat. Chem. Biol 17 (4) (2021) 465–476. [PubMed: 33542532]

[45]. Chen D, et al. , iPLA2β-mediated lipid detoxification controls p53-driven ferroptosis independent of GPX4, Nat. Commun 12 (1) (2021) 1–15. [PubMed: 33397941]

[46]. Vázquez-Medina JP, et al. , Genetic inactivation of the phospholipase A(2) activity of peroxiredoxin 6 in mice protects against LPS-induced acute lung injury, Am. J. Physiol. Lung Cell Mol. Physiol 316 (4) (2019) L656–l668. [PubMed: 30702344]

[47]. Vázquez-Medina JP, et al. , The phospholipase A2 activity of peroxiredoxin 6 modulates NADPH oxidase 2 activation via lysophosphatidic acid receptor signaling in the pulmonary endothelium and alveolar macrophages, Faseb. J 30 (8) (2016) 2885–2898. [PubMed: 27178323]

[48]. Li P, et al. , Glutathione peroxidase 4–regulated neutrophil ferroptosis induces systemic autoimmunity, Nat. Immunol 22 (9) (2021) 1107–1117. [PubMed: 34385713]

[49]. Wu Q, et al. , Macrophages originated IL-33/ST2 inhibits ferroptosis in endometriosis via the ATF3/SLC7A11 axis, Cell Death Dis. 14 (10) (2023) 668.

[50]. Divakaruni AS, et al., Analysis and interpretation of microplate-based oxygen consumption and pH data, in: Methods in Enzymology, Elsevier, 2014, pp. 309–354.

[51]. Söderberg O, et al. , Direct observation of individual endogenous protein complexes in situ by proximity ligation, Nat. Methods 3 (12) (2006) 995–1000. [PubMed: 17072308]

[52]. Söderberg O, et al. , Characterizing proteins and their interactions in cells and tissues using the in situ proximity ligation assay, Methods 45 (3) (2008) 227–232. [PubMed: 18620061]

[53]. Livak KJ, Schmittgen TD, Analysis of relative gene expression data using realtime quantitative PCR and the 2(-Delta Delta C(T)) Method, Methods 25 (4) (2001) 402–408. [PubMed: 11846609]

[54]. Subramanian A, et al. , Gene set enrichment analysis: a knowledge-based approach for interpreting genome-wide expression profiles, Proc. Natl. Acad. Sci. USA 102 (43) (2005) 15545–15550. [PubMed: 16199517]

[55]. Wu G, Feng X, Stein L, A human functional protein interaction network and its application to cancer data analysis, Genome Biol. 11 (5) (2010) R53. [PubMed: 20482850]

[56]. Wu G, Haw R, Functional interaction network construction and analysis for disease discovery, Methods Mol. Biol 1558 (2017) 235–253. [PubMed: 28150241]

[57]. Wang J, et al. , WebGestalt 2017: a more comprehensive, powerful, flexible and interactive gene set enrichment analysis toolkit, Nucleic Acids Res. 45 (W1) (2017) W130–W137. [PubMed: 28472511]

[58]. Janky R, et al. , iRegulon: from a gene list to a gene regulatory network using large motif and track collections, PLoS Comput. Biol 10 (7) (2014) e1003731. [PubMed: 25058159]

[59]. Wang Y, et al. , Lung injury and mortality with hyperoxia are increased in peroxiredoxin 6 gene-targeted mice, Free Radic. Biol. Med 37 (11) (2004) 1736–1743. [PubMed: 15528033]

[60]. Wang Y, et al. , Peroxiredoxin 6 gene-targeted mice show increased lung injury with paraquat-induced oxidative stress, Antioxidants Redox Signal. 8 (1–2) (2006) 229–237.

[61]. Wang Y, et al. , Transgenic mice overexpressing peroxiredoxin 6 show increased resistance to lung injury in hyperoxia, Am. J. Respir. Cell Mol. Biol 34 (4) (2006) 481–486. [PubMed: 16399955]

[62]. Dixon SJ, et al. , Pharmacological inhibition of cystine–glutamate exchange induces endoplasmic reticulum stress and ferroptosis, Elife 3 (2014) e02523. [PubMed: 24844246]

[63]. Manevich Y, Feinstein SI, Fisher AB, Activation of the antioxidant enzyme 1-CYS peroxiredoxin requires glutathionylation mediated by heterodimerization with πGST, Proc. Natl. Acad. Sci. U.S.A 101 (11) (2004) 3780–3785. [PubMed: 15004285]

[64]. Conrad M, Sato H, The oxidative stress-inducible cystine/glutamate antiporter, system xc–: cystine supplier and beyond, Amino Acids 42 (2012) 231–246. [PubMed: 21409388]

[65]. Miura K, et al. , Cystine uptake and glutathione level in endothelial cells exposed to oxidative stress, Am. J. Physiol. Cell Physiol 262 (1) (1992) C50–C58.

[66]. Skouta R, et al. , Ferrostatins inhibit oxidative lipid damage and cell death in diverse disease models, J. Am. Chem. Soc 136 (12) (2014) 4551–4556. [PubMed: 24592866]

[67]. Fang X, et al. , Ferroptosis as a target for protection against cardiomyopathy, Proc. Natl. Acad. Sci. USA 116 (7) (2019) 2672–2680. [PubMed: 30692261]

[68]. Meng Z, et al. , HMOX1 upregulation promotes ferroptosis in diabetic atherosclerosis, Life Sci. 284 (2021) 119935. [PubMed: 34508760]

[69]. Chen X, et al. , Ferroptosis: machinery and regulation, Autophagy (2020) 1–28. [PubMed: 31516068]

[70]. Xue X, et al. , Iron uptake via DMT1 integrates cell cycle with JAK-STAT3 signaling to promote colorectal tumorigenesis, Cell Metabol. 24 (3) (2016) 447–461.

[71]. Li N, et al. , Ferritinophagy-mediated ferroptosis is involved in sepsis-induced cardiac injury, Free Radic. Biol. Med 160 (2020) 303–318. [PubMed: 32846217]

[72]. Soula M, et al. , Metabolic determinants of cancer cell sensitivity to canonical ferroptosis inducers, Nat. Chem. Biol 16 (12) (2020) 1351–1360. [PubMed: 32778843]

[73]. Li S, et al. , Iron overload in endometriosis peritoneal fluid induces early embryo ferroptosis mediated by HMOX1, Cell Death Discov. 7 (1) (2021) 1–12.

[74]. Meadows SM, Myers CT, Krieg PA, Regulation of endothelial cell development by ETS transcription factors, in: Seminars in Cell & Developmental Biology, Elsevier, 2011.

[75]. Wang LC, et al. , Yolk sac angiogenic defect and intra-embryonic apoptosis in mice lacking the Ets-related factor TEL, EMBO J. 16 (14) (1997) 4374–4383. [PubMed: 9250681]

[76]. Blattler A, et al. , ZBTB33 binds unmethylated regions of the genome associated with actively expressed genes, Epigenet. Chromatin 6 (1) (2013) 1–18.

[77]. Daniel JM, et al. , The p120 ctn-binding partner Kaiso is a bi-modal DNA-binding protein that recognizes both a sequence-specific consensus and methylated CpG dinucleotides, Nucleic Acids Res. 30 (13) (2002) 2911–2919. [PubMed: 12087177]

[78]. De Braekeleer E, et al. , ETV6 fusion genes in hematological malignancies: a review, Leuk. Res 36 (8) (2012) 945–961. [PubMed: 22578774]

[79]. Gerak CA, et al. , Biophysical characterization of the ETV6 PNT domain polymerization interfaces, J. Biol. Chem 296 (2021).

[80]. Kim CA, et al. , Polymerization of the SAM domain of TEL in leukemogenesis and transcriptional repression, EMBO J. 20 (15) (2001) 4173–4182. [PubMed: 11483520]

[81]. Prokhortchouk A, et al. , The p120 catenin partner Kaiso is a DNA methylation-dependent transcriptional repressor, Genes Dev. 15 (13) (2001) 1613–1618. [PubMed: 11445535]

[82]. Pozner A, Terooatea TW, Buck-Koehntop BA, Cell-specific Kaiso (ZBTB33) regulation of cell cycle through cyclin D1 and cyclin E1, J. Biol. Chem 291 (47) (2016) 24538–24550. [PubMed: 27694442]

[83]. Koh D-I, et al. , Transcriptional activation of APAF1 by KAISO (ZBTB33) and p53 is attenuated by RelA/p65, Biochimica et Biophys. Acta (BBA)-Gene Regul. Mech 1849 (9) (2015) 1170–1178.

[84]. Maillet A, Pervaiz S, Redox regulation of p53, redox effectors regulated by p53: a subtle balance, Antioxidants Redox Signal. 16 (11) (2012) 1285–1294.

[85]. Tarangelo A, et al. , p53 suppresses metabolic stress-induced ferroptosis in cancer cells, Cell Rep. 22 (3) (2018) 569–575. [PubMed: 29346757]

[86]. Speckmann B, et al. , Induction of glutathione peroxidase 4 expression during enterocytic cell differentiation, J. Biol. Chem 286 (12) (2011) 10764–10772. [PubMed: 21252226]

[87]. Huang H-S, Chen C-J, Chang W-C, The CCAAT-box binding factor NF-Y is required for the expression of phospholipid hydroperoxide glutathione peroxidase in human epidermoid carcinoma A431 cells, FEBS Lett. 455 (1–2) (1999) 111–116. [PubMed: 10428483]

[88]. Nguyen HP, et al. , Aifm2, a NADH oxidase, supports robust glycolysis and is required for cold-and diet-induced thermogenesis, Mol. Cell 77 (3) (2020) 600–617. e4. [PubMed: 31952989]

[89]. Wang L, et al. , ATF3 promotes erastin-induced ferroptosis by suppressing system Xc–, Cell Death Differ. 27 (2) (2020) 662–675. [PubMed: 31273299]

[90]. Lan C, et al. , Suppression of IRF9 promotes osteoclast differentiation by decreased ferroptosis via STAT3 activation, Inflammation (2023) 1–15.

[91]. Rodencal J, et al. , Sensitization of cancer cells to ferroptosis coincident with cell cycle arrest, Cell Chem. Biol (2023).

[92]. Santesmasses D, Gladyshev VN, Selenocysteine machinery primarily supports TXNRD1 and GPX4 functions and together they are functionally linked with SCD and PRDX6, Biomolecules 12 (8) (2022) 1049. [PubMed: 36008942]

[93]. Paluchova V, et al. , The role of peroxiredoxin 6 in biosynthesis of FAHFAs, Free Radic. Biol. Med 193 (2022) 787–794. [PubMed: 36403738]

[94]. Gao M, et al. , Role of mitochondria in ferroptosis, Mol. Cell 73 (2) (2019) 354–363. e3. [PubMed: 30581146]

[95]. López-Grueso MJ, et al. , Knockout of PRDX6 induces mitochondrial dysfunction and cell cycle arrest at G2/M in HepG2 hepatocarcinoma cells, Redox Biol. 37 (2020) 101737. [PubMed: 33035814]

[96]. Ingold I, et al. , Selenium utilization by GPX4 is required to prevent hydroperoxide-induced ferroptosis, Cell 172 (3) (2018) 409–422. e21. [PubMed: 29290465]

[97]. Wortmann M, et al. , Combined deficiency in glutathione peroxidase 4 and vitamin E causes multiorgan thrombus formation and early death in mice, Circ. Res 113 (4) (2013) 408–417. [PubMed: 23770613]

[98]. Hu Q, et al. , GPX4 and vitamin E cooperatively protect hematopoietic stem and progenitor cells from lipid peroxidation and ferroptosis, Cell Death Dis. 12 (7) (2021) 1–9. [PubMed: 33414393]

[99]. Akiba S, et al. , Characterization of acidic Ca2+-independent phospholipase A2 of bovine lung, Comp. Biochem. Physiol. B Biochem. Mol. Biol 120 (2) (1998) 393–404. [PubMed: 9787801]

[100]. Feinstein SI, Mouse models of genetically altered peroxiredoxin 6, Antioxidants 8 (4) (2019) 77. [PubMed: 30934692]

[101]. Mao C, et al. , Phospholipase iPLA2β Acts as a Guardian against Ferroptosis, Wiley Online Library, 2021.

[102]. Luo P, et al. , Celastrol induces ferroptosis in activated HSCs to ameliorate hepatic fibrosis via targeting peroxiredoxins and HO-1, Acta Pharm. Sin. B (2021).

[103]. Zhang Q, et al. , Sp1-mediated upregulation of Prdx6 expression prevents podocyte injury in diabetic nephropathy via mitigation of oxidative stress and ferroptosis, Life Sci. 278 (2021) 119529. [PubMed: 33894270]

[104]. Yang WS, Stockwell BR, Synthetic lethal screening identifies compounds activating iron-dependent, nonapoptotic cell death in oncogenic-RAS-harboring cancer cells, Chem. Biol 15 (3) (2008) 234–245. [PubMed: 18355723]

[105]. Vučković AM, et al. , Inactivation of the glutathione peroxidase GPx4 by the ferroptosis-inducing molecule RSL3 requires the adaptor protein 14-3-3ε, FEBS Lett. 594 (4) (2020) 611–624. [PubMed: 31581313]

[106]. Sorokina EM, et al. , Mutation of serine 32 to threonine in peroxiredoxin 6 preserves its structure and enzymatic function but abolishes its trafficking to lamellar bodies, J. Biol. Chem 291 (17) (2016) 9268–9280. [PubMed: 26921317]

[107]. Sorokina EM, et al. , Intracellular targeting of peroxiredoxin 6 to lysosomal organelles requires MAPK activity and binding to 14-3-3ε, Am. J. Physiol. Cell Physiol 300 (6) (2011) C1430–C1441. [PubMed: 21346153]

[108]. Sorokina EM, et al. , Identification of the amino acid sequence that targets peroxiredoxin 6 to lysosome-like structures of lung epithelial cells, Am. J. Physiol. Lung Cell Mol. Physiol 297 (5) (2009) L871–L880. [PubMed: 19700648]

[109]. Li Z, et al. , Ribosome stalling during selenoprotein translation exposes a ferroptosis vulnerability, Nat. Chem. Biol 18 (7) (2022) 751–761. [PubMed: 35637349]

[110]. Ralat LA, et al. , Direct evidence for the formation of a complex between 1-cysteine peroxiredoxin and glutathione S-transferase π with activity changes in both enzymes, Biochemistry 45 (2) (2006) 360–372. [PubMed: 16401067]

[111]. Wainberg M, et al. , A genome-wide atlas of co-essential modules assigns function to uncharacterized genes, Nat. Genet 53 (5) (2021) 638–649. [PubMed: 33859415]

[112]. Ma S, et al. , Peroxiredoxin 6 is a crucial factor in the initial step of mitochondrial clearance and is upstream of the PINK1-parkin pathway, Antioxidants Redox Signal. 24 (9) (2016) 486–501.

[113]. Min Y, et al. , Peroxiredoxin-6 negatively regulates bactericidal activity and NF-κB activity by interrupting TRAF6-ECSIT complex, Front. Cell. Infect. Microbiol 7 (2017) 94. [PubMed: 28393051]

[114]. Eismann T, et al. , Peroxiredoxin-6 protects against mitochondrial dysfunction and liver injury during ischemia-reperfusion in mice, Am. J. Physiol. Gastrointest. Liver Physiol 296 (2) (2009) G266–G274. [PubMed: 19033532]

[115]. Wang Y, et al. , SLC25A39 is necessary for mitochondrial glutathione import in mammalian cells, Nature 599 (7883) (2021) 136–140. [PubMed: 34707288]

[116]. Nomura K, et al. , Mitochondrial phospholipid hydroperoxide glutathione peroxidase suppresses apoptosis mediated by a mitochondrial death pathway, J. Biol. Chem 274 (41) (1999) 29294–29302. [PubMed: 10506188]

[117]. Nomura K, et al. , Mitochondrial phospholipid hydroperoxide glutathione peroxidase inhibits the release of cytochrome c from mitochondria by suppressing the peroxidation of cardiolipin in hypoglycaemia-induced apoptosis, Biochem. J 351 (Pt 1) (2000) 183–193. [PubMed: 10998361]

[118]. Jelinek A, et al. , Mitochondrial rescue prevents glutathione peroxidase-dependent ferroptosis, Free Radic. Biol. Med 117 (2018) 45–57. [PubMed: 29378335]

[119]. Tadokoro T, et al. , Mitochondria-dependent ferroptosis plays a pivotal role in doxorubicin cardiotoxicity, JCI Insight 5 (9) (2020).

[120]. Jang S, et al. , Elucidating the contribution of mitochondrial glutathione to ferroptosis in cardiomyocytes, Redox Biol. (2021) 102021. [PubMed: 34102574]

[121]. Takashi Y, et al. , Mitochondrial dysfunction promotes aquaporin expression that controls hydrogen peroxide permeability and ferroptosis, Free Radic. Biol. Med 161 (2020) 60–70. [PubMed: 33017631]

[122]. Rath S, et al. , MitoCarta3. 0: an updated mitochondrial proteome now with suborganelle localization and pathway annotations, Nucleic Acids Res. 49 (D1) (2021) D1541–D1547. [PubMed: 33174596]

[123]. Guo X, et al. , Mitochondrial stress is relayed to the cytosol by an OMA1–DELE1–HRI pathway, Nature 579 (7799) (2020) 427–432. [PubMed: 32132707]

[124]. Quirós PM, et al. , Multi-omics analysis identifies ATF4 as a key regulator of the mitochondrial stress response in mammals, JCB (J. Cell Biol.) 216 (7) (2017) 2027–2045. [PubMed: 28566324]

[125]. Lim JK, et al. , Cystine/glutamate antiporter xCT (SLC7A11) facilitates oncogenic RAS transformation by preserving intracellular redox balance, Proc. Natl. Acad. Sci. USA 116 (19) (2019) 9433–9442. [PubMed: 31000598]

[126]. Lu S, et al. , ATF3 contributes to brucine-triggered glioma cell ferroptosis via promotion of hydrogen peroxide and iron, Acta Pharmacol. Sin (2021) 1–13.

[127]. McComb S, et al. , Type-I interferon signaling through ISGF3 complex is required for sustained Rip3 activation and necroptosis in macrophages, Proc. Natl. Acad. Sci. USA 111 (31) (2014) E3206–E3213. [PubMed: 25049377]

[128]. Man SM, Karki R, Kanneganti TD, Molecular mechanisms and functions of pyroptosis, inflammatory caspases and inflammasomes in infectious diseases, Immunol. Rev 277 (1) (2017) 61–75. [PubMed: 28462526]

[129]. Dai X-G, et al. , The interaction between C/EBPβ and TFAM promotes acute kidney injury via regulating NLRP3 inflammasome-mediated pyroptosis, Mol. Immunol 127 (2020) 136–145. [PubMed: 32971400]

[130]. Li H, et al. , The interferon signaling network and transcription factor C/EBP-β, Cell. Mol. Immunol 4 (6) (2007) 407. [PubMed: 18163952]

[131]. Proneth B, Conrad M, Ferroptosis and necroinflammation, a yet poorly explored link, Cell Death Differ. 26 (1) (2019) 14–24. [PubMed: 30082768]

[132]. Sun Y, et al. , The emerging role of ferroptosis in inflammation, Biomed. Pharmacother 127 (2020) 110108. [PubMed: 32234642]

[133]. Liao P, et al. , CD8+ T cells and fatty acids orchestrate tumor ferroptosis and immunity via ACSL4, Cancer Cell 40 (4) (2022) 365–378. e6. [PubMed: 35216678]

[134]. Patel P, Chatterjee S, Peroxiredoxin6 in endothelial signaling, Antioxidants 8 (3) (2019) 63. [PubMed: 30871234]

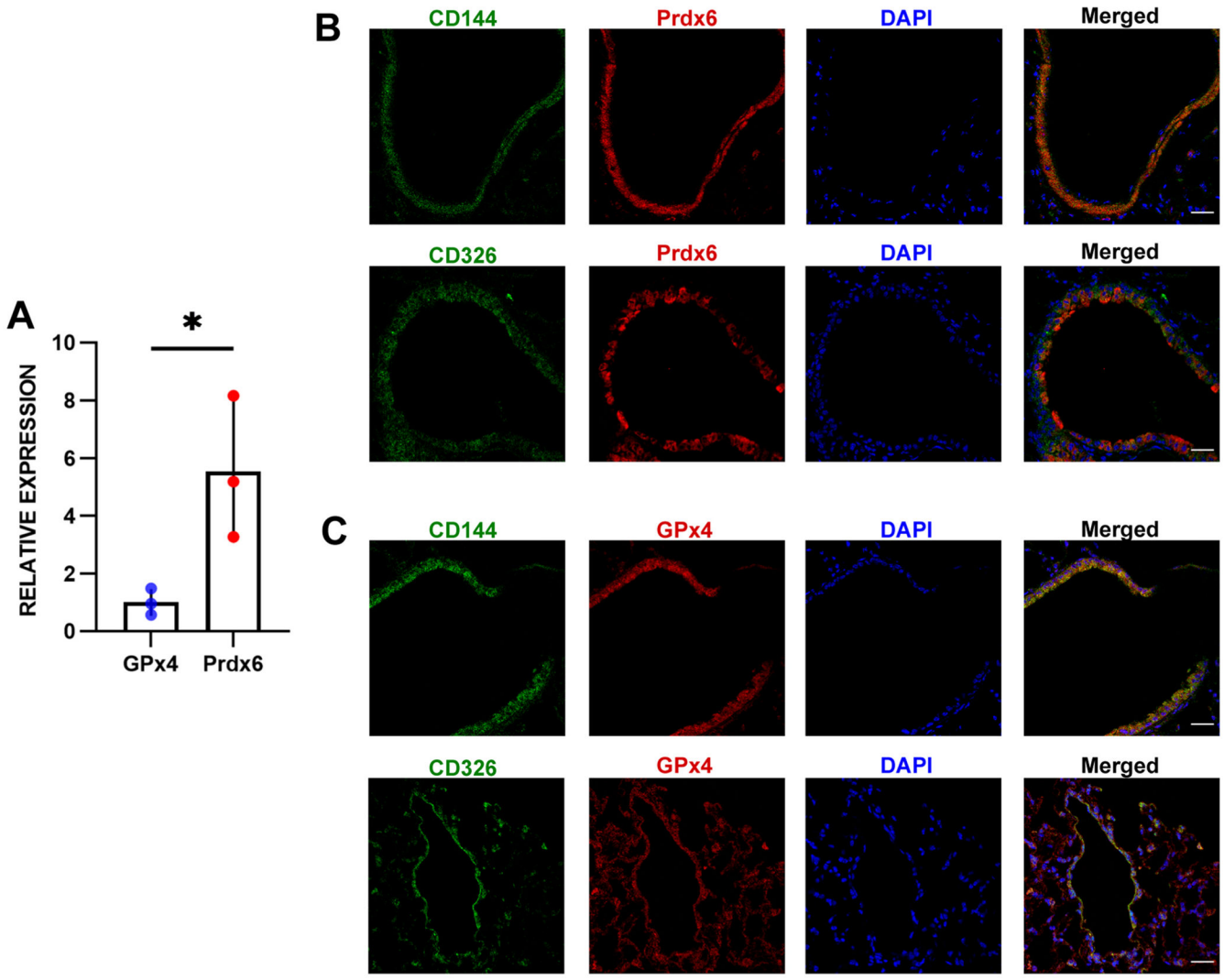

Fig. 1. Prdx6 is a widely expressed lung phospholipid hydroperoxide GSH peroxidase.

A) mRNA levels of Prdx6 and GPx4 in whole murine lungs ($t = 3.137$, $^*p = 0.034$). B) Prdx6 and C) GPx4 co-localization with vascular endothelial cadherin (CD144) and epithelial cell adhesion molecule (CD326) in mouse lungs. Scale bar is 25 μm.

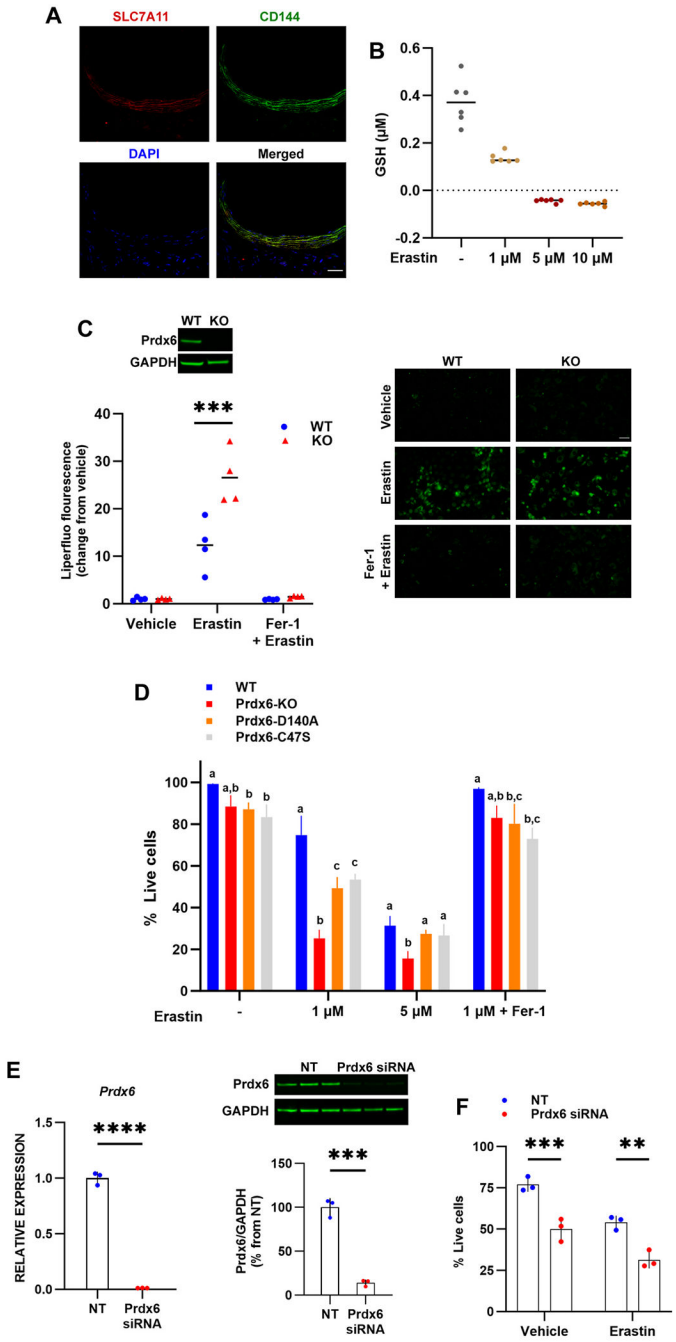

Fig. 2. Prdx6 deficiency sensitizes lung endothelial cells to ferroptosis.

A) SLC7A11 co-localization with vascular endothelial cadherin (CD144) in mouse lungs. Scale bar is 25 μm. B) GSH levels in MPMVECs treated with increasing erastin concentrations for 24 h. C) Lipid peroxidation in WT and Prdx6 KO MPMVECs treated with 1 μM erastin with and without 1 μM ferrostatin-1 (Fer-1, 1 μM) for 24 h. Liperfluo (10 μM) was added in the last hour of the incubation period. Scale bar is 50 μm. D) Erastin-induced, Fer-1 dependent cell death in WT, Prdx6 KO and Prdx6 KI MPMVECs. Cells were treated with erastin with or without Fer-1 and evaluated for cell viability and

cytotoxicity. Different letters denote significant strain differences within each treatment. E) Prdx6 KD in HPMVECs. F) Effect of Prdx6 KD on cell death in HPMVECs treated with and without 1 μM erastin for 24 h. NT: non-targeting siRNA. Data are mean ± SD of at least three independent experiments. * = $p < 0.05$, ** = $p < 0.01$, *** = $p < 0.001$, **** = $p < 0.0001$.

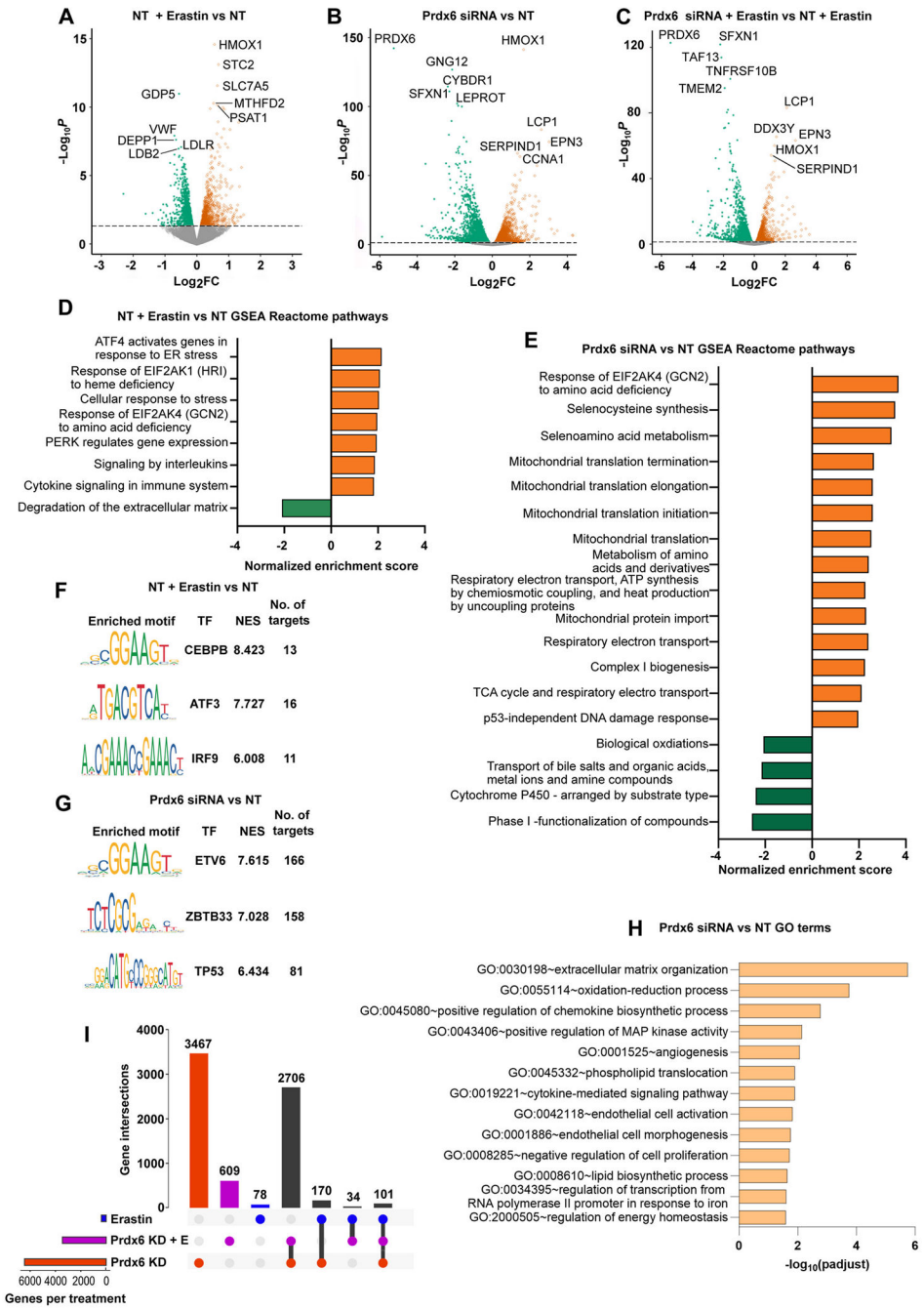

Fig. 3. Prdx6 deficiency upregulates transcriptional signatures of selenoamino acid metabolism and mitochondrial function.

A) Volcano plot showing differentially expressed (DE) genes in HPMVECs transfected with NT siRNAs and treated with 1 μM erastin for 24 h. B) DE genes in cells with Prdx6 KD. C) DE genes in cells transfected with NT or Prdx6-targeting siRNAs and treated with erastin. D) GSEA of Reactome pathways enriched in cells transfected with NT siRNAs and treated with erastin. E) GSEA of Reactome pathways enriched in Prdx6 KD cells. *Cis*-regulatory elements analysis in F) cells transfected with NT siRNAs and treated with erastin and G) Prdx6 KD cells. H) Gene ontology (GO) terms enriched in Prdx6 KD cells. I) UpSet plots

of DE genes in cells with and without Prdx6 KD and erastin treatment. NT: non-targeting siRNAs. NES = normalized enriched score. TF = transcription factor. Data are from three independent experiments. FDR = 5%.

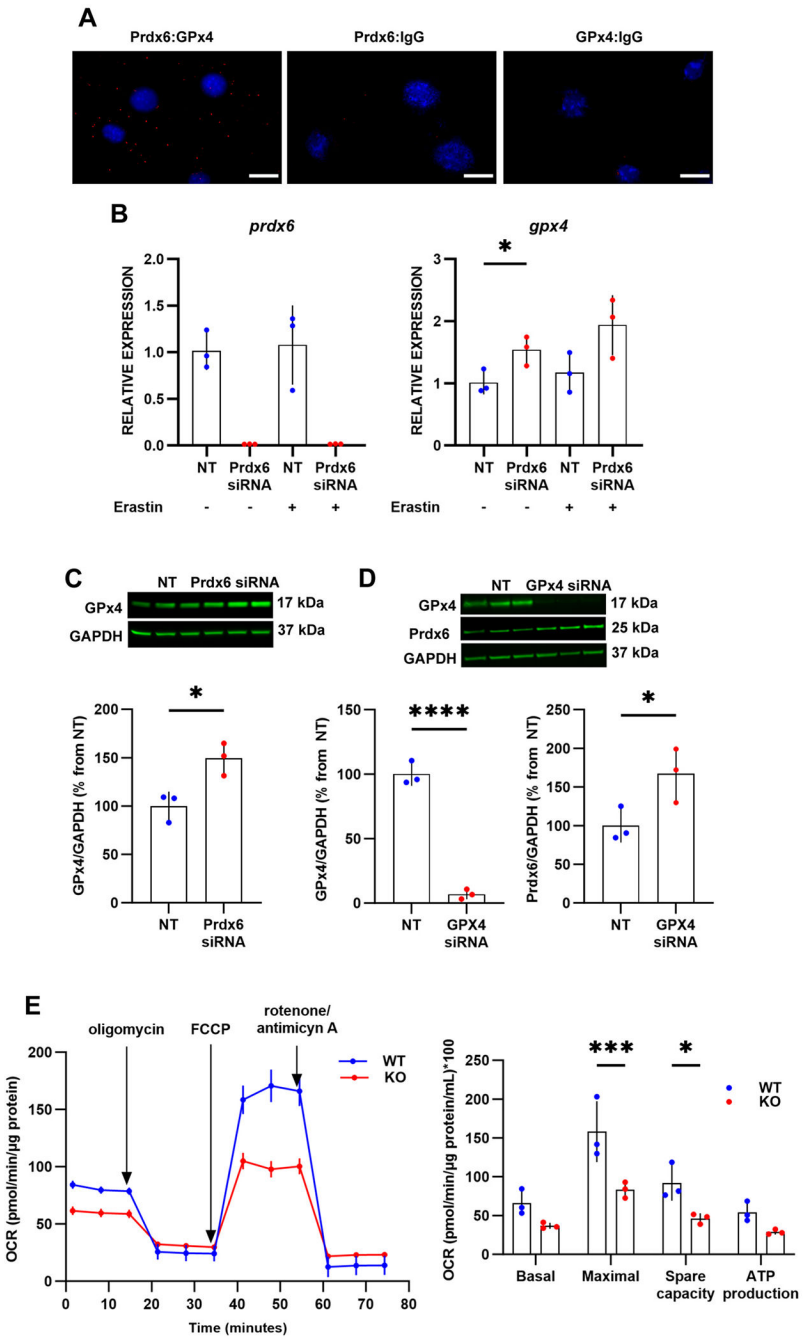

Fig. 4. Prdx6 deficiency increases expression and abundance of the selenoprotein GPx4 while suppressing mitochondrial function.

A) Prdx6:GPx4 interactions detected using in situ proximity ligation in intact HPMVECs. Red puncta indicate close proximity (<40 nm) of the 2 proteins. Nuclei are counterstained with DAPI. Scale bar is 25 µm. B) Prdx6 and GPx4 mRNA levels in HPMVECs with Prdx6 KD with and without erastin treatment. C) GPx4 abundance in HPMVECs with Prdx6 KD. D) Effect of GPx4 KD on Prdx6 abundance in HPMVECs. Data are mean ± SD of at least three independent experiments. E) Oxygen consumption rates (OCR) and mitochondrial

function in WT and Prdx6 KO MPMVECs. Data shown are replicates from an experiment that was repeated three times. * = $p < 0.05$, *** = $p < 0.001$, **** = $p < 0.0001$.